Mps1 promotes poleward chromosome movements in meiotic prometaphase

Régis E. Meyer[a,*], Aaron R. Tipton[a], Rebecca LaVictoire[a], Gary J. Gorbsky[a,b], and Dean S. Dawson[a,b,*]

[a]Program in Cell Cycle and Cancer Biology, Oklahoma Medical Research Foundation, [b]Department of Cell Biology, University of Oklahoma Health Sciences Center, Oklahoma City, OK 73104

ABSTRACT **In prophase of meiosis I, homologous chromosomes pair and become connected by cross-overs. Chiasmata, the connections formed by cross-overs, enable the chromosome pair, called a bivalent, to attach as a single unit to the spindle. When the meiotic spindle forms in prometaphase, most bivalents are associated with one spindle pole and then go through a series of oscillations on the spindle, attaching to and detaching from microtubules until the partners of the bivalent become bioriented—attached to microtubules from opposite sides of the spindle. The conserved kinase, Mps1, is essential for the bivalents to be pulled by microtubules across the spindle in prometaphase. Here we show that *MPS1* is needed for efficient triggering of the migration of microtubule-attached kinetochores toward the poles and promotes microtubule depolymerization. Our data support the model Mps1 acts at the kinetochore to coordinate the successful attachment of a microtubule and the triggering of microtubule depolymerization to then move the chromosome.**

Monitoring Editor
Kerry Bloom
University of North Carolina, Chapel Hill

Received: Aug 11, 2020
Revised: Mar 1, 2021
Accepted: Mar 12, 2021

INTRODUCTION

In many organisms, cells enter prometaphase of meiosis with improper kinetochore-microtubule attachments that would lead to segregation errors if they were not corrected (Nicklas, 1997; Meyer *et al.*, 2013; Chmátal *et al.*, 2015). In budding yeast each partner chromosome in the homologue pair (called a bivalent) can attach one microtubule to its kinetochore (Winey *et al.*, 2005; Sarangapani *et al.*, 2014). The bivalents begin meiosis mono-oriented (both partners at one pole) and, through a series of steps, become bioriented and prepared to separate away from each other at anaphase I (Figure 1A). The microtubule-organizing centers, called spindle pole bodies (SPBs) in yeast, are duplicated in premeiotic S-phase resulting in an older SPB and a newly formed SPB. In late prophase the homologous chromosome pairs (called bivalents) cluster at the side-by-side SPBs in a microtubule-dependent manner (Figure 1A). The end of prophase and entry into prometaphase is marked by the formation of a spindle between the SPBs, forcing them apart with the bivalents attached mainly to the older SPB. The bivalents are released from this monopolar attachment in an Aurora B–dependent manner (Monje-Casas *et al.*, 2007; Meyer *et al.*, 2013) as was previously demonstrated in mitotic cells (Biggins *et al.*, 1999; Cheeseman *et al.*, 2002; Tanaka *et al.*, 2002). Then, following a series of migrations back and forth across the spindle that include a series of microtubule releases (via Aurora B) and reattachments, the partners of the bivalents become attached to microtubules from opposite SPBs (Meyer *et al.*, 2013). During this process, the spindle assembly checkpoint senses the state of kinetochore-microtubule attachments and delays cell cycle progression into anaphase until all chromosome pairs are bioriented (Shonn *et al.*, 2000; Cheslock *et al.*, 2005).

The process of attaching the kinetochores to microtubules appears to be controlled at several levels (reviewed in Tanaka, 2010; Godek *et al.*, 2015; Lampson and Grishchuk, 2017). A series of studies from the Tanaka laboratory defined these steps in yeast mitosis (Figure 1B). They found that, in yeast, as in other organisms, the kinetochores first attach most often to lateral surfaces of microtubules (Hayden *et al.*, 1990; Merdes and De Mey, 1990;

This article was published online ahead of print in MBoC in Press (http://www.molbiolcell.org/cgi/doi/10.1091/mbc.E20-08-0525-T) on March 31, 2021.

Author contributions: Conceptualization, R.E.M. and D.S.D.; methodology, R.E.M., A.R.T., and D.S.D.; investigation, R.E.M., A.R.T., R. L., and D.S.D.; writing, R.E.M. and D.S.D.; manuscript review and editing, all authors; supervision, G.J.G. and D.S.D.; funding acquisition, G.J.G. and D.S.D.

*Address correspondence to: Dean S. Dawson (dawsond@omrf.org); Régis E. Meyer (regis-meyer@omrf.org).

Abbreviation used: SPB, spindle pole body.

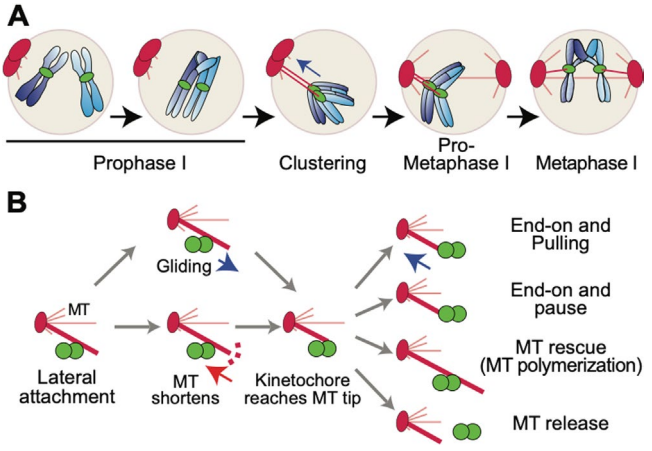

FIGURE 1: Kinetochore-microtubule interactions in budding yeast meiosis. (A) In prophase I, chromosomes have released their attachments to microtubules. At the exit from prophase I, centromeres cluster at the side-by-side SPBs. When SPBs separate to form a spindle, most centromeres are attached to the older SPB. Following a period of oscillations on the spindle including microtubule releases and reattachments, the homologous partners become bioriented. (B) Studies in mitotic cells suggest that most initial attachments are lateral (adapted from Tanaka, 2010). Microtubules depolymerize until they meet the kinetochore. In some organisms, kinetochores can glide toward the microtubule plus end. When the microtubule plus end meets the kinetochore, the illustrated outcomes have been observed.

Rieder and Alexander, 1990; Tanaka *et al.*, 2005; Franco *et al.*, 2007; Gachet *et al.*, 2008; Magidson *et al.*, 2011). Second, the microtubule depolymerizes to bring the microtubule plus end to the kinetochore (Kitamura *et al.*, 2007; Tanaka *et al.*, 2007). The kinetochore and microtubule plus end can then have any of several fates (Figure 1B). The microtubule can repolymerize, the kinetochore can release the microtubule, or the kinetochore can form an end-on attachment that can move the kinetochore poleward as the microtubule depolymerizes. In this process, the protein composition at the kinetochore-microtubule interface, and modifications of those proteins, change, which promotes the ability of the kinetochore to track the shortening microtubule (Asbury *et al.*, 2006; Westermann *et al.*, 2006; Grishchuk *et al.*, 2008; Daum *et al.*, 2009; Gaitanos *et al.*, 2009; Powers *et al.*, 2009; Welburn *et al.*, 2009; Lampert *et al.*, 2010; Schmidt *et al.*, 2012; Volkov *et al.*, 2013; Umbreit *et al.*, 2014).

Mps1 is a conserved kinase with a central role in the spindle assembly checkpoint (Hardwick *et al.*, 1996; Weiss and Winey, 1996; Abrieu *et al.*, 2001). In budding yeast, Mps1 also has an essential role in meiotic chromosome segregation (Straight *et al.*, 2000). An analysis of the role of the Mps1 in meiosis revealed that it was needed for the efficient poleward migration of centromeres during the biorientation process (Figure 1A) (Meyer *et al.*, 2013). In addition, Mps1 is needed for an efficient spindle checkpoint in meiosis I. In *MPS1* mutants, following anaphase I, most chromosomes end up associated with the spindle pole with which they were initially associated when the spindle first formed (Meyer *et al.*, 2013). This is because they cannot move across the spindle to the opposite pole in prometaphase. Because most chromosomes connect to the older SPB just before prometaphase, even in wild-type cells, *MPS1* mutants exhibit more than 80% nondisjunction, nearly all to the older SPB at anaphase I. The Ipl1 kinase, but not Mps1, is critical for releasing these monopolar attachments and for controlling the restructuring of kinetochores in meiosis prophase, but is not critical for poleward migration during prometaphase of meiosis I (Miller *et al.*, 2012; Meyer *et al.*, 2013, 2015; Chen *et al.*, 2020).

This role of Mps1 in promoting force-generating kinetochore-microtubule attachments is critical for meiosis but less so in mitosis (Meyer *et al.*, 2013). In budding yeast as in many other organisms, *MPS1* is an essential gene, but separation-of-function alleles have been identified that result in severe defects in meiotic biorientation but very mild defects in mitosis (Meyer *et al.*, 2013). This suggests either that meiosis is particularly sensitive to defects in the biorientation machinery, or alternatively, that meiotic sensitivity to *MPS1* mutations reflects a meiosis-specific process. Interestingly, similar meiosis-specific mutant alleles of *MPS1* have also been isolated in *Drosophila* and zebrafish (Poss *et al.*, 2004; Gilliland *et al.*, 2005).

The manner in which Mps1 promotes the formation of force-generating attachments between kinetochores and microtubule plus ends is unclear. Does Mps1 promote the movement of kinetochores toward the spindle midzone so they can encounter microtubules from the opposite pole, or convert lateral attachments to end-on attachments, or stabilize end-on kinetochore-microtubule attachments, or trigger microtubule depolymerization to drag kinetochores poleward (Figure 1B)? Because Mps1 kinase is known to have many targets, it could be involved in coordinating multiple steps in the biorientation process. Here we use live cell imaging experiments to explore the meiotic roles of Mps1. The results of these experiments suggest that *MPS1* mutants can form end-on kinetochore-microtubule attachments but these mutants are defective in the subsequent microtubule depolymerization that pulls kinetochores poleward.

RESULTS

Mps1 is necessary for chromosome movements across the meiotic spindle

Previous work has shown that Mps1 is needed for the efficient establishment of force-generating attachments of kinetochores to microtubules. This is a multistep process (Figure 1B), and the step, or steps, at which *MPS1* mutants are defective is unknown. Therefore, we used live cell imaging to track chromosome movements at various stages of the meiotic biorientation process in order to identify the deficiencies that occur when *MPS1* is inactive.

We focused on the *mps1-R170S* mutation because this separation-of-function allele has only mild mitotic defects and severe meiotic defects, thus providing clues as to the critical roles that Mps1 plays in meiosis. As a control, we used an analogue-sensitive allele that allowed us to inactivate the Mps1 kinase activity with an ATP analogue (*mps1-as1*) (Jones *et al.*, 2005). Prior studies revealed that both mutations result in high levels of meiosis I nondisjunction (Meyer *et al.*, 2013). To track chromosome movement, one chromosome (chromosome I) was tagged adjacent to its centromere with an array of *lac* operator repeats, and the cells expressed lacI-GFP, which binds to the repeats, from a meiotic promotor (Straight *et al.*, 1996). The movement of this GFP-tagged centromere was tracked in cells with a deletion of *SPO11*. In this background, homologous partner chromosomes do not become connected by recombination events to form bivalents (Figure 2A) (Klapholz *et al.*, 1985; Loidl *et al.*, 1994). The resulting partnerless univalents, each with only one kinetochore, can never biorient on the spindle and thus go through repeated cycles of microtubule attachment, migration on the spindle, and microtubule detachment (Figure 2B) (Meyer *et al.*, 2013). Using this assay, both *mps1-as1* and *mps1-R170S* mutants exhibit a considerable loss in the ability of chromosomes to traverse across the spindle, while in wild-type cells the GFP-tagged chromosome

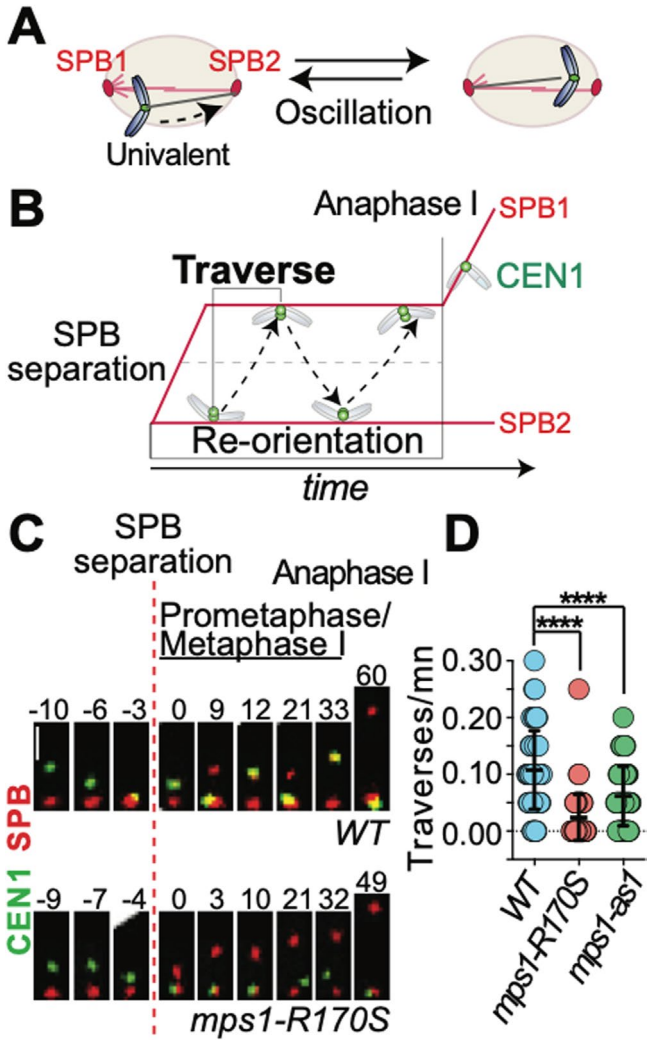

FIGURE 2: Mps1 promotes migration across the meiotic spindle. (A) Cartoon illustrating the process of re-orientation in the absence of links between homologues (*spo11Δ* background). As the univalent does not have the ability to biorient, it will reorient indefinitely. (B) The reorientation process in the *spo11* background can be evaluated by quantifying the traverses of a GFP-tagged centromere across the spindle. (C, D) *spo11Δ* diploid cells, with the indicated genotypes, with one GFP-tagged *CEN1* and the SPB marker (*SPC42-DsRed*) were sporulated and released from a pachytene arrest (P_{GAL1}-*NDT80 GAL4-ER*) at 6 h after meiotic induction by the addition of 5 μM β-estradiol. The experiment was performed in three biological replicates, and 20 cells were scored in each replicate of the experiment. The pooled data from the three replicates (60 cells for each genotype) are presented. Images were collected at 45 s (one replicate) or 2 min (two replicates) intervals for 75 min. Representative kymographs from wild-type and *msp1-R170S* cells are shown. Scale bar: 2 μm. (D) For each cell, the number of traverses was recorded for the first 20 min after the spindle formed. The data (as traverses/minute) for each cell are plotted. Error bars are the average and SD for each set of 60 cells; ****$p < 0.0001$ (ordinary one-way analysis of variance [ANOVA], multiple comparisons).

crosses the spindle, on average, about once every 6 min during prometaphase (Figure 2, C and D).

The coupling of kinetochores to the plus ends of depolymerizing microtubules is presumably the major driving force for the poleward movements that occur on bipolar spindles. However, in assays with bipolar spindles (as in Figure 2C) it is difficult to know exactly how the kinetochore of a particular chromosome is attached to a microtubule. The rapid and processive migrations across the midzone and to the opposite pole are most consistent with the kinetochore being dragged by a depolymerizing plus end–attached microtubule toward the spindle pole where its minus end is attached (Tanaka *et al.*, 2007). However, it is formally possible that these movements could be gliding of the centromere along the side of a microtubule in the opposite direction, away from the SPB and toward the plus end of the microtubule it is tracking (Figure 1B) (Kapoor *et al.*, 2006; Windecker *et al.*, 2009; Akera *et al.*, 2015).

To examine the directionality of chromosome movements on microtubules in meiosis, we assayed the movements of a univalent chromosome (*spo11* background) on the monopolar microtubule array that emanates from the side-by-side SPBs as cells exit pachytene (Figures 1A and 3A). On these monopolar arrays, all poleward movements of chromosomes are minus end directed and all movements away from the pole are toward the microtubule plus ends. In this experiment, cells were released from a prophase arrest and chromosome movements on the monopolar array were monitored (Figure 3, A–C). In cells expressing the wild-type *MPS1* gene the univalents migrated toward the side-by-side SPBs (clustering) in consecutive cycles (Figure 3, B and C) and as cells approached the time of spindle assembly, GFP-tagged centromeres were more and more likely to have become positioned against the SPBs (Supplemental Figure S1). The beginning of clustering, about 30 min before spindle assembly, may correspond to the time at which new Ndc80 complexes, capable of interacting with microtubule plus ends, are added to the meiotic kinetochore (Miller *et al.*, 2012; Meyer *et al.*, 2015; Chen *et al.*, 2020). This clustering does not occur in *ndc80-md* mutants that cannot produce new outer kinetochores after exiting prophase, arguing that the movements depend on kinetochore-microtubule interactions (Supplemental Figure S1). The majority of wild-type cells cluster the GFP-tagged centromere 5–10 min before spindle assembly, while clustering is significantly delayed in the *MPS1* mutants (Figure 3D). Further, the length of time centromeres spent at the SPBs during the consecutive cycles of clustering is shorter in *MPS1* mutants (Figure 3E). Similar observations were obtained by monitoring bivalent pairs (*SPO11*) (Supplemental Figure S2). The trend in these experiments is for centromeres to migrate toward the minus ends of microtubules in an *MPS1* and *NDC80*–dependent manner. Although we cannot visualize individual kinetochore-microtubule attachments in these experiments, the data are consistent with the model that Mps1 is needed to promote minus end–directed locomotion, via Ndc80-mediated attachments to the plus ends of microtubules to get the centromeres to the SPBs. They do not eliminate the possibility that there is also a plus-ended gliding process in budding yeast meiosis. Indeed, this could be one of the forces that moves the centromeres away from the SPBs in the repeated cycles of clustering.

mps1-R170S mutants exhibit pausing defects during the biorientation process

The imaging experiments above (and a prior characterization of Mps1 in meiosis (Meyer *et al.*, 2013), employ relatively long frame intervals (from 45 s to 2 min) to allow acquisition of data for cells proceeding from prometaphase thru anaphase I without photobleaching or toxicity. At this frame rate, a traverse of a centromere across the entire spindle can occur in the interval between sequential frames and details about pauses, restarts, and reversals of direction that occur as the kinetochore interacts with a microtubule are not detected. Understanding these details might clarify at which

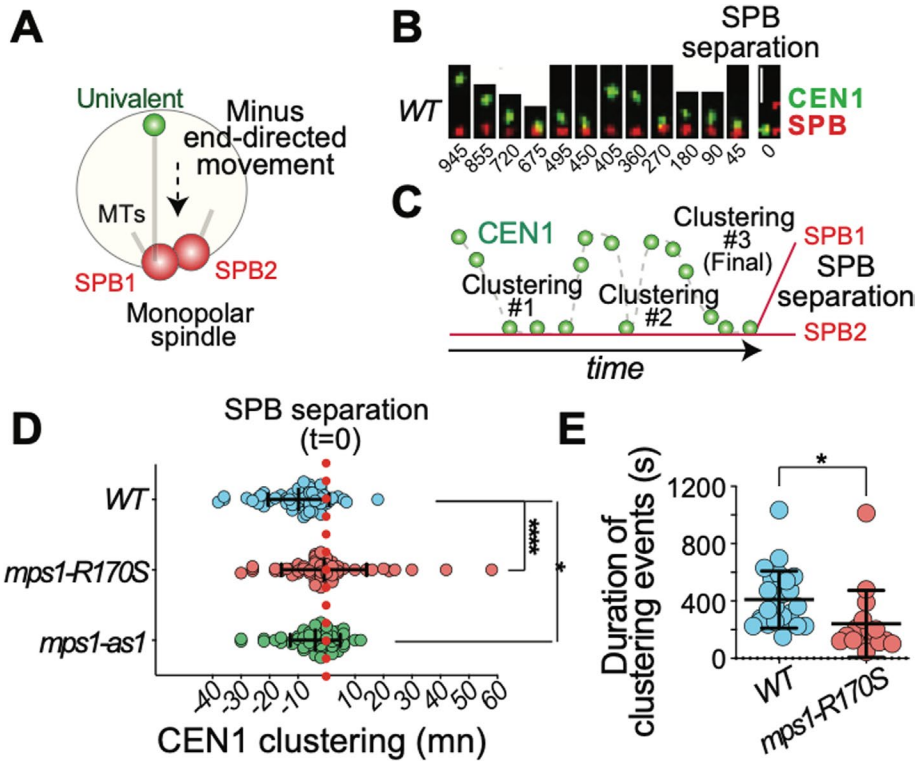

FIGURE 3: Mps1 promotes minus end–directed migration to the base of monopolar microtubule arrays. (A) Schematic representation of centromere clustering on a monopolar microtubule array. (B) Images of a representative wild-type cell exhibiting cycles of clustering of GFP-tagged *CEN1* (green) at the side-by-side SPBs (red) before spindle formation (the last image). Scale bar: 2 µm. (C) The pulling of the chromosome can be separated in two alternating phases where *CEN1* is either moving toward the SPBs (Clustering) or at a relative constant distance from the SPBs. (D) Clustering of GFP-tagged *CEN1* was monitored using live cell imaging of *spo11Δ* diploid cells with *MPS1*, *mps1-R170S*, or *mps1-as1* alleles. Experiments were performed in three biological replicates imaged at 45 s (once) or 2 min (twice) frame rates. The graph shows the timing of the final clustering of *CEN1* (within 0.5 µm) relative to the time of SPB separation for each individual cell. The red dotted line represents the time at which the SPBs separated. *$p < 0.05$, ****$p < 0.0001$ (ordinary one-way ANOVA, multiple comparisons). (E) *MPS1* and *mps1-R170S* cells from the 45 s frame rate replicate were evaluated to determine the amount of time that *CEN1* was positioned at the side-by-side SPBs (within 0.5 µm) in individual cells in the 45 min preceding SPB separation to make the prometaphase spindle (duration of clustering). The total time that *CEN1* was at the SPBs in each cell is shown ($n = 25$ cells for the wild-type control and $n = 16$ cells for *mps1-R170S*; unpaired *t* test, *$p < 0.05$).

steps in the biorientation process Mps1 is playing a critical function. To identify smaller-scale chromosome movements that occur within a single traverse, we imaged chromosome behavior at much faster acquisition rates (2 s intervals) over the course of 5 min, again using a *spo11* mutant background so the resulting green fluorescent protein (GFP)-tagged chromosome I univalent could not become biioriented. Images were acquired using a Thru-focus method in which a single image is collected as the objective lens focuses thru the cell (Conrad *et al.*, 2008). Deconvolution of the acquired data then produces a two-dimensional projection of the image. To reduce acquisition times, the SPBs and the centromere of chromosome I were both tagged with GFP.

Chromosome behavior was quantified in cells with bipolar spindles. In control cells expressing wild-type *MPS1*, chromosomes exhibited several behaviors during the 5 min "snapshots" of prometaphase. We assigned these behaviors to five categories (Figure 4A). These included 1) clustering at one SPB, 2) maintaining a position between the poles (nonpolar), 3) low-mobility half spindle—small movements within one half spindle, 4) high mobility—directed movements, toward or away from the SPB but not moving across the entire spindle, and 5) traverses across the spindle. In most wild-type cells the centromere exhibited at least one traverse or half spindle–length migration in a 5 min window of prometaphase (Figure 4A, iv and v). These high-mobility movements were greatly reduced in *mps1-R170S* mutants (Figure 4A, iv and v). In contrast, it was uncommon in the wild-type control strain for centromeres to linger in a nonpolar position (Figure 4Aii), but this occurred significantly more frequently in *mps1-R170S* mutants where it was the predominant category. Furthermore, the centromeres scored as "nonpolar" in *mps1-R170S* cells appeared more stationary than those in wild-type cells (Figure 4B). To quantify this, we plotted the positions of the GFP-tagged centromere relative to the SPBs in every frame of the 5 min movie (150 frames) (Figure 4C). Representative traces of the GFP-tagged centromeres in a wild-type cell, a *dam1-md* mutant (which is defective in maintaining end-on kinetochore attachments [Meyer *et al.*, 2018]) and three *mps1-R170S* cells show that in the *mps1-R170S* mutants the centromeres appear locked-in-place (Figure 4C). We quantified all of the movements of centromeres in the nonpolar category (Figure 4Aii) by determining the median position of each centromere over the 5 min movie and then determining the distance of the centromere from that position in each of the 150 frames (Figure 4D, cartoon). The data for wild-type cells, *mps1-R170S* mutant cells, and *ndc80-md* mutant cells (in which centromeres are left at the spindle midzone, consistent with a failure to form productive end-on kinetochore-microtubule attachments) are shown in Figure 4D. This analysis reveals that in *mps1-R170S* cells the centromere stays within a smaller area during prometaphase than is observed in wild-type cells (Figure 4D). Furthermore, *mps1-R170S* centromeres exhibit significantly more very short movements (less than 100 nm)—note that the spindle length in these experiments is about 2 µm (Figure 4E).

mps1-R170S mutants exhibit reduced processivity during poleward centromere migrations

The static behavior of the nonpolar centromeres in *mps1-R170S* mutants is consistent with the model that they represent kinetochores that are attached to the ends of microtubules that are not depolymerizing. This could be analogous to the "paused" kinetochore-microtubule attachments observed in mitotic budding yeast cells by the Tanaka laboratory (Tanaka *et al.*, 2005. 2007; Tanaka, 2010) that sometimes occur when a microtubule depolymerizes until it meets a laterally attached kinetochore (Figure 1B). The elevated numbers of the static nonpolar centromeres in *mps1-R170S* cells numbers are consistent with the model that one role of Mps1 is to phosphorylate

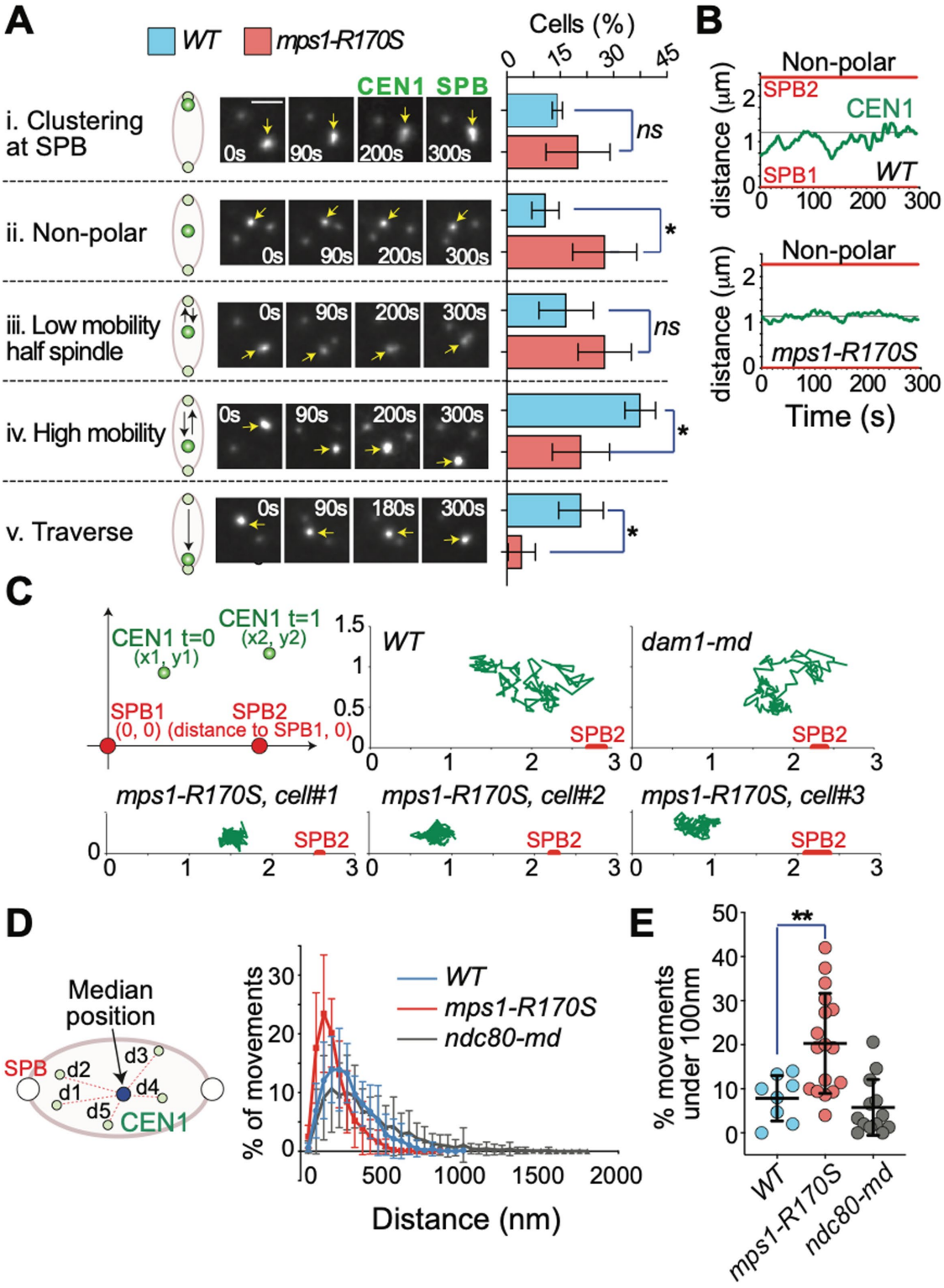

FIGURE 4: Mps1 promotes chromosome mobility on the meiotic prometaphase spindle. (A–C) *spo11Δ* diploid cells, with the indicated genotypes, with one *CEN1-GFP*–tagged chromosome and a SPB marker (*SPC42-GFP*) were sporulated and released from a pachytene arrest (P_{GAL1}-*NDT80 GAL4-ER*) at 6 h after introduction to sporulation medium by the addition of 5 μM β-estradiol. Subsequently, cells were harvested and observed by time-lapse imaging during meiosis at 2 s intervals for 5 min. Chromosomes were scored in cells with 1.5–3.5-μm-long spindles (cells in prometaphase–metaphase [Meyer *et al.*, 2013]). The experiment was performed as three biological replicates per genotype with 40 cells scored per replicate. (A) Cells were placed in one of five categories according to the primary behavior of the GFP-tagged centromere during the 5 min interval: clustered (remaining close to one SPB), nonpolar (positioned away from the poles and not migrating toward a pole), low-mobility half spindle (making small movements within one half spindle), high mobility (moving poleward or toward the midzone, covering a distance of approximately

targets at the end-on attached kinetochore-microtubule interface to help convert paused kinetochores to moving kinetochores. To investigate this model, we characterized the behavior of centromeres making poleward migrations in wild-type and *mps1-R170S* cells. We identified centromeres that in the course of our 5 min snapshot of prometaphase moved from a position that was about 1 micron (0.9–1.2 μm) away from a spindle pole toward that pole (Figure 5A). Such cells are rare in the *mps1-R170S* population due to the preponderance of locked-in-place centromeres. These poleward migrations could come from either pushing or pulling forces, but because the migrations occur within a half spindle (the average spindle length was more than 2 microns) they are presumably mediated most often by minus end–directed movements along a microtubule that emanates from the destination pole (Figure 5A). The chart of the movements of each tracked centromere as it moves poleward (Figure 5B) reveals first, that all centromeres exhibit some reversals and pauses during the journey. Some of these might be artifactual as 1) the measurements are taken from two-dimensional projections of three-dimensional spindles so spindle rotations in the Z-dimension could distort the true kinetochore-SPB distance, and 2) the movements are relatively small compared with the sizes of the centromere GFP and SPB foci—distances measured are from the center of each focus. Measuring protocols were used to minimize these issues (see *Materials and Methods*). Tracking the individual centromeres showed that poleward migrations took significantly less time in wild-type cells than in *mps1-R170S* mutants (Figure 5, B and C). To determine whether this was because centromeres reach higher velocities in wild-type cells, we measured the velocities of both poleward and anti-poleward centromere movements over the course of migrations to the pole (Figure 5D). Measurements were obtained as a sliding three-frame window (4 s) in which the centromere moved in the same direction between frames 1 and 2 and between frames 2 and 3. There was no obvious difference in the average speeds of either poleward or anti-poleward movements of the GFP-tagged centromere in wild-type and *mps1-R170S* strains; the velocities exhibited by the GFP-tagged centromere as it made poleward migrations were indistinguishable (Figure 5D; average forward velocity, WT 76.23 nm/s, $n = 13$, *mps1-R170S* 58.80 nm/s, $n = 15$; $p = 0.0758$; average reverse velocity, WT 38.58 nm/s, $n = 12$, *mps1-R170S* 41.33 nm/s, $n = 15$; $p = 0.65$, unpaired *t* tests). If the centromere movements during poleward migration are driven mainly by microtubule depolymerization, then kinetochore microtubule depolymerization occurs at indistinguishable rates in wild-type cells and *mps1-R170S* mutants.

Because migration to the pole takes much longer in *mps1-R170S* mutants than in wild-type cells but the velocities of poleward movements are indistinguishable, this argues that the *mps1-R170S* mutants must pause or reverse more often. To test this, we measured the frequency with which the GFP-tagged centromere paused or reversed direction in its poleward migration (Figure 5E). The *MPS1* mutants exhibited significantly more pauses, or reversals of direction, in their journeys to the pole (Figure 5F), and the distance traveled between pauses or reversals was significantly shorter (Figure 5G). Because the velocities of movement in wild-type cells and *mps1-R170S* mutants are indistinguishable, the higher numbers of pauses in *MPS1* mutants results in longer times for poleward journeys of centromeres in these cells.

If Mps1 acts during prometaphase to promote depolymerization of kinetochore microtubules, and kinetochore microtubules are stabilized in *MPS1* mutants, then microtubule turnover should be reduced in prometaphase in *MPS1* mutants (Figure 6A). To test this, we measured microtubule turnover in cells expressing a photoconvertible mEos2-tagged α-tubulin subunit (Markus *et al.*, 2015). mEos2-Tub1 has properties of a GFP until it is pulsed with 405 nm light, at which point it switches to a red fluorescent protein (RFP) (Figure 6B). To measure turnover of kinetochore microtubules, we pulsed half of the spindle of cells expressing mEos2-Tub1 with 405 nm light and then measured turnover of the red fluorescent signal (Table 1). Previous measurements of microtubule turnover in budding yeast have been in mitotic cells, but the majority of defects we have examined with *MPS1* mutants have been in meiotic cells. Therefore, we first compared microtubule turnover in metaphase spindles of yeast meiotic and mitotic cells and found them to be indistinguishable (Figure 6C). To confirm that our methods could detect variations in microtubule turnover rates in meiosis, we measured turnover in cells expressing an auxin-degradable version of the microtubule plus-end protein Stu2 (Stu2-AID*), which helps to regulate microtubule dynamics in mitotic metaphase (Wolyniak *et al.*, 2006; Podolski *et al.*, 2014; Miller *et al.*, 2016; Humphrey *et al.*, 2018; Miller *et al.*, 2019). Cells were induced to enter meiosis, and microtubule turnover was measured in the presence or absence of auxin. As observed previously in mitotic cells, (Kosco *et al.*, 2001; Pearson *et al.*, 2003), inactivating Stu2 in meiotic cells reduced microtubule turnover (Figure 6D). If Mps1 is, like Stu2, promoting microtubule turnover in metaphase cells, then inactivating Mps1 should give a similar outcome. To test this, we compared microtubule turnover in metaphase meiotic wild-type cells and *mps1-as1* cells (both in the presence of the Mps1-as1 inhibitor 1-NMPP1). Microtubule turnover rates in metaphase, with or without Mps1 activity, were indistinguishable. This finding is consistent with the reduction in Mps1 levels at kinetochores as they become bioriented and the spindle checkpoint is satisfied (Dou *et al.*, 2003; Howell *et al.*, 2004; Aravamudhan *et al.*, 2015; Koch *et al.*, 2019). Our failure to

one-fourth to three-fourths of a spindle length, and traverse (moving pole-to-pole across the entire spindle). Examples of each classification are shown. Scale bar: 2 μm. *$p < 0.05$ (unpaired *t* tests). (B) Traces of the position of *CEN1* relative to the SPBs from representative wild-type and *mps1-R170S* cells that were classified as "non-polar" in panel A. (C) The top left panel is a schematic of the relative positions of the GFP-tagged *CEN1* in two sequential imaging frames (SPBs are shown in red). The spindle-centered reference system has three key parameters: The position of SPB1 is constant at $x = 0$ and $y = 0$, the position of SPB2 depends on the spindle length (variable over time), and the coordinates *x* and *y* (in microns) define the distance of *CEN1* from SPB1 at that imaging frame. Shown are traces of the location of *CEN1*, relative to the SPBs, in 150 sequential time points (every 2 s for 5 min) in five representative cells from the nonpolar category. (D, E) Detailed analysis of centromeres exhibiting nonpolar behavior. (D) We calculated the median position of *CEN1* over the course of the 5 min imaging period and then determined the distance of *CEN1* from that median position (nanometers) for each frame (150 total) of the acquisition (see cartoon). The graph shows the distribution of distances (in 100 nm bins) from the mean centromere position per cell. The error bars represent the average and SD. $n = 8$ cells for WT, 17 cells for *mps1-R170S*, and 13 cells for *ndc80-md*. (E) The proportion of individual *CEN1* movements (in D) that were less than 100 nm from the median position was calculated for each indicated genotype. Mutant genotypes were compared with the wild-type control. **$p < 0.01$ (ordinary one-way ANOVA).

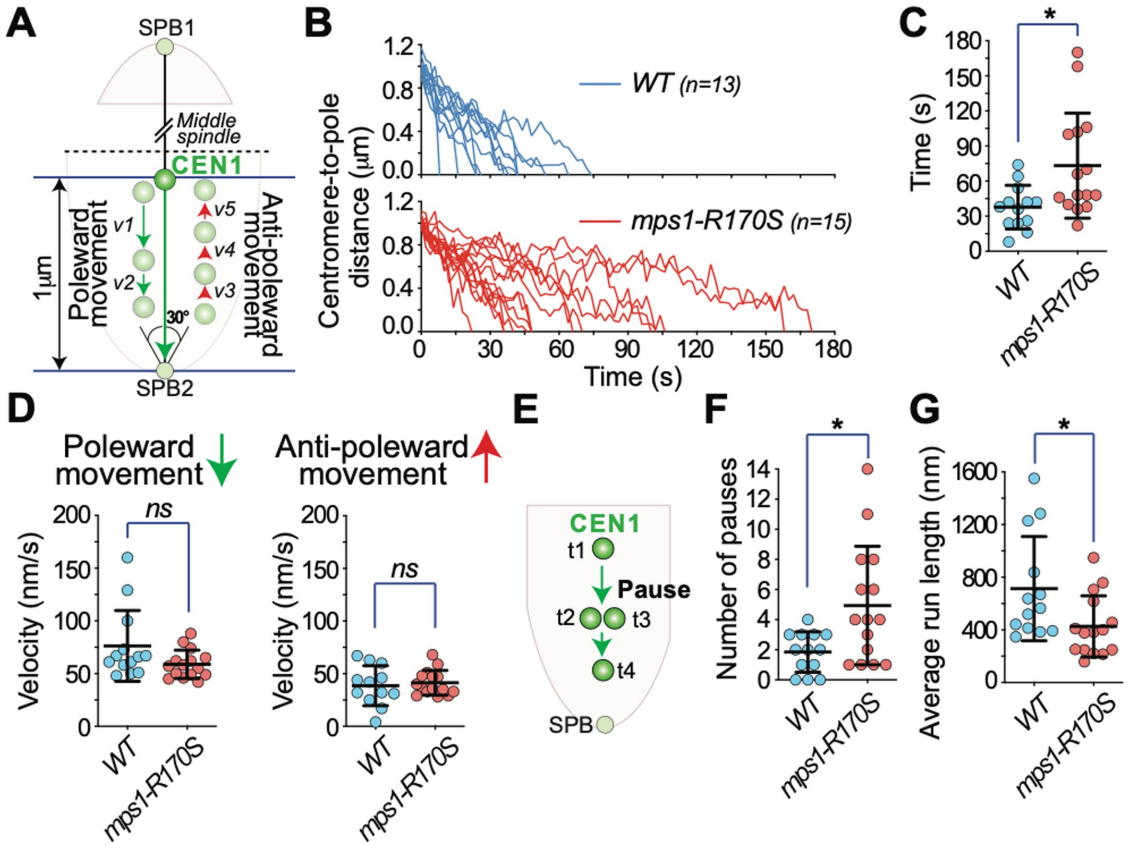

FIGURE 5: Mps1 is required for processive poleward migration in prometaphase. (A) We identified cells in which the GFP-tagged *CEN1* migrated across the middle of the spindle and proceeded to the opposite pole, moving along the central axis of the spindle (within 15° of the axis from the destination SPB). Frame-to-frame movements (both poleward and anti-poleward) for the final 1 micron of the migration were quantified. The *MPS1* cells came from two isogenic cultures while the *mps1-R170S* cells came from four isogenic cultures. (B) Charts of the poleward movement of *CEN1* for wild-type (blue) and *mps1-R170S* mutant (red) cells. $T = 0$ represents the time *CEN1* is 1 micron from the SPB and is moving toward the nearest pole. (C) Graph of the cells in B showing the time spent for each *CEN1* migrating to the SPB from 1 micron away (WT: 37.69 s ± SD 18.71, $n = 13$; *mps1-R170S*: 73.20 s ± SD 44.91, $n = 15$, $^*p < 0.05$, unpaired *t* test). The 1 μm migrations in B could be divided into shorter continuous poleward or anti-poleward movements in which the GFP-tagged *CEN1* tracked in the same direction in continuous frames separated by frames in which the *CEN1* paused or reversed. (D) The distribution of the velocities of the incremental poleward (left) or anti-poleward (right) *CEN1* movements measured during the 1 micron poleward migration. (E) Cartoon illustrating the pauses or reversals of direction of *CEN1* movement observed during the 1 micron poleward migrations. (F) Graph showing the number of pauses or changes of direction for each individual 1 micron poleward migration of *CEN1* (WT 1.85 ± SD 1.35, $n = 13$; *mps1-R170S*: 4.93 ± SD 3.93, $n = 15$, $^*p < 0.05$, Student's *t* test). (G) The average distances traveled by the GFP-tagged *CEN1* between pauses/reversals (WT 713.2 nm ± SD 396.1, $n = 13$; *mps1-R170S*: 425.6 nm ± 232.4, $n = 15$, $^*p < 0.05$, unpaired *t* test).

detect a role for Mps1 in metaphase microtubule dynamics could suggest that it is simply not involved in that function. The meiotic defects we have observed in *MPS1* mutants were in prometaphase, before chromosomes are bioriented, raising the question of whether microtubule dynamics are discernibly different in prometaphase and metaphase cells using our microtubule turnover assay. In wild-type yeast meiosis, most of the chromosomes are bioriented within a few minutes after spindle formation (Meyer *et al.*, 2013). Therefore, we used the *spo11* mutation to obtain a population of cells in which none of the chromosomes are bioriented. Consistent with the higher rates of turnover for unattached versus stably attached kinetochore microtubules (Gorbsky and Borisy, 1989; Zhai *et al.*, 1995), the spindles in the *spo11* cells exhibited higher rates of microtubule turnover than were seen in metaphase cells (Figure 6, B and F). If Mps1 promotes depolymerization of the kinetochore microtubules of non-bioriented chromosomes in prometaphase, then this higher rate of turnover seen in prometaphase should be reduced in *MPS1* mutants. For both *mps1-as1* and *mps1-R170S* this proved to be the case (Figure 6, G and H). Both mutations reduce the rate of turnover to levels like those seen in metaphase cells, where inactivating Mps1 has no discernible effect on microtubule turnover.

DISCUSSION

Previous work has shown that Mps1 is essential for proper chromosome segregation in meiosis in a variety of organisms (Straight *et al.*, 2000; Poss *et al.*, 2004; Gilliland *et al.*, 2005). We have found that, in budding yeast meiosis, Mps1 impacts at least three steps in the biorientation process (Meyer *et al.*, 2013, 2018). First, Mps1 promotes the migration of bivalents to the side-by-side SPBs at the base of a monopolar microtubule array following the exit from meiotic prophase (clustering). Second, Mps1 promotes the processive poleward movements on the prometaphase meiosis I spindle that occur

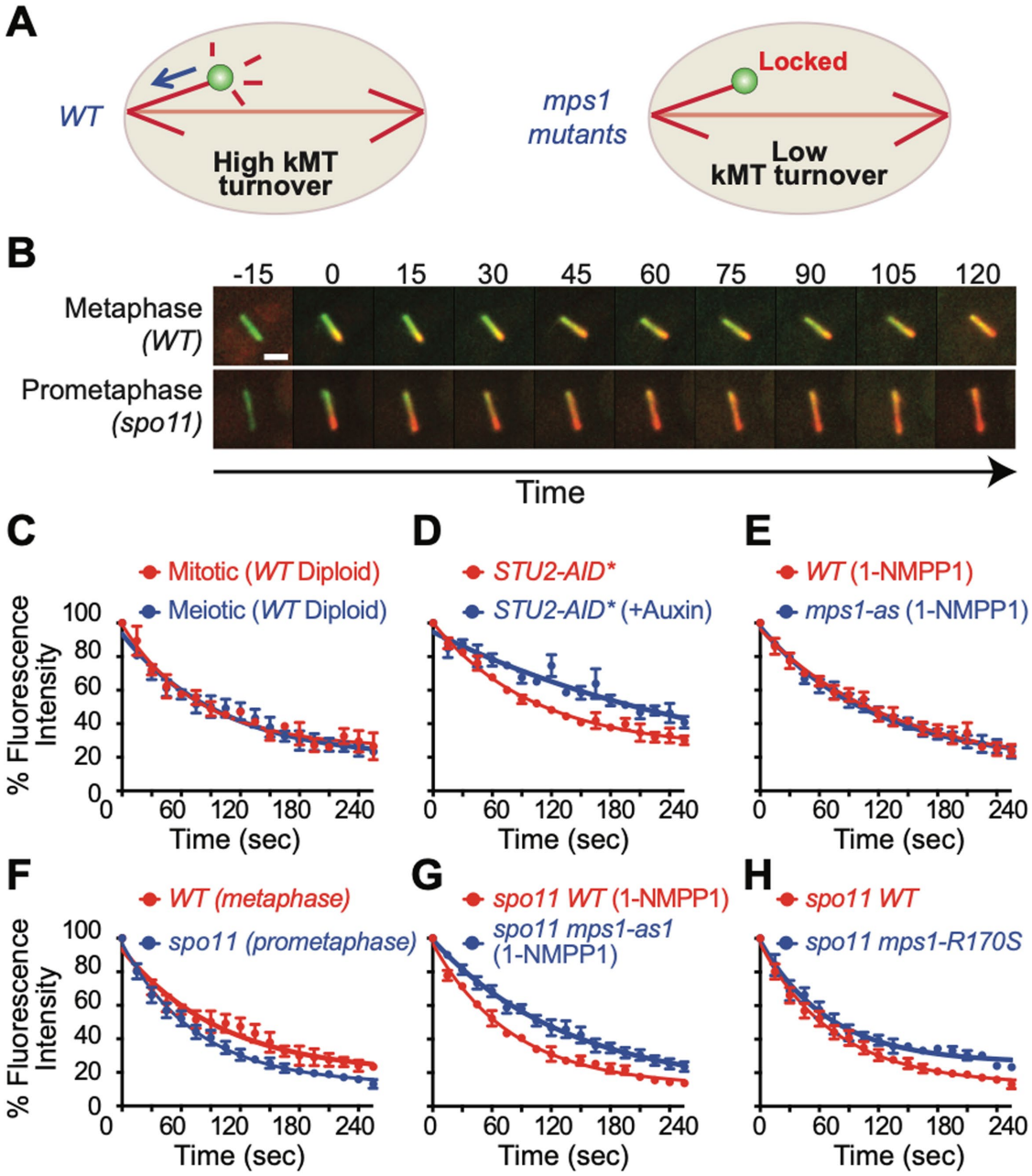

FIGURE 6: Mps1 promotes microtubule turnover in meiotic prometaphase. (A) In wild-type cells the shortening kinetochores of actively biorienting chromosomes are predicted to cause a high microtubule turnover. *MPS1* mutants exhibit a locked-in-place phenotype that might represent a defect in the depolymerization of kinetochore microtubules. (B) Cells that were unable to form bipolar attachments (*spo11*), and thus in a prolonged prometaphase-like state, were used to measure microtubule turnover. Half spindles of meiotic cells were pulsed with 405 nm light to photoconvert mEos2-Tub1 (from green to red). Images were acquired every 15 s, and the intensity of the red signal was measured (see *Materials and Methods*). Scale bar: 2 μm. (C) Microtubule turnover on metaphase spindles was measured in a diploid strain undergoing either meiosis or mitosis. (D) Microtubule turnover was measured in cells expressing *STU2-AID** in the presence or absence of auxin and $CuSO_4$ (copper was used to induce expression of the P_{CUP1}-*AFB2* F-box protein construct). (E) Microtubule turnover was measured on meiotic metaphase spindles of wild-type or *mps1-as1* cells in the presence of the Mps1-as1 inhibitor 1-NMPP1. (F) Microtubule turnover was measured on meiotic metaphase and prometaphase spindles of wild-type cells. (G) Microtubule turnover was measured on prometaphase spindles (*spo11*) in cells with or without the inactivation of Mps1 by 1-NMPP1. (H) Microtubule turnover was measured on prometaphase spindles (*spo11*) in wild-type or *mps1-R170S* cells. All experiments show the averages and SEM of three or more biological replicates with three or more cells per replicate (see Table 1).

before bivalents become bioriented. Third, through phosphorylation of Dam1, and possibly other targets, Mps1 helps to stabilize end-on attachments of the prometaphase kinetochores to microtubules.

The failure of *MPS1* mutants to phosphorylate Dam1 does not explain the massive defects in meiotic chromosome segregation exhibited by *MPS1* mutants. Despite their defects in kinetochore-

Type of cells	Stage	# of replicates	# of cells	Half-time ($t_{1/2}$; s)	Spindle length (μm)	R^2
WT	Mitotic metaphase	3	10 (4, 3, 3)	119.5	nd	0.938
WT	Meiotic metaphase	4	25 (7, 6, 6, 6)	119.5	2.69	0.961
WT *(1-NMPP1)*	Meiotic metaphase	3	26 (8, 12, 6)	126.0	2.62	0.986
mps1-as1 (1-NMPP1)	Meiotic metaphase	4	29 (8, 5, 7, 9)	133.3	3.55	0.986
*STU2-AID**	Meiotic metaphase	3	29 (10, 12, 7)	135.9	2.46	0.973
STU2-AID (+Auxin)*	Meiotic metaphase	3	23 (11, 4, 8)	223.6	2.15	0.945
spo11	Meiotic prometaphase	3	35 (9, 13, 13)	79.7	3.34	0.979
spo11 mps1-R170S	Meiotic prometaphase	3	25 (8, 10, 7)	115.5	3.11	0.932
spo11 (1-NMPP1)	Meiotic prometaphase	3	20 (6, 7, 7)	80.6	3.59	0.981
spo11 mps1-as1 (1-NMPP1)	Meiotic prometaphase	4	29 (8, 8, 4, 9)	119.5	3.09	0.995

TABLE 1: Microtubule turnover measurements.

microtubule interactions, *dam1-2A* mutants that cannot be phosphorylated by Mps1 exhibit rather mild meiotic chromosome segregation defects (Shimogawa *et al.*, 2006; Meyer *et al.*, 2018). Thus, there must be another role (or roles) of Mps1 that explains its essentiality for meiotic chromosome segregation. Our experiments have not revealed a critical meiotic substrate but have refined our understanding of the ways in which Mps1 affects chromosome dynamics in meiosis I.

Our results suggest that the major defect in *MPS1* mutants is in regulating microtubule dynamics at the kinetochore interface. A number of observations point to this conclusion. First, when kinetochores are moving poleward in *MPS1* mutants, the average velocity is indistinguishable from that of wild-type cells (Figure 5D). This suggests that Mps1 is not essential for kinetochores to track depolymerizing microtubules. In addition, it demonstrates that once a kinetochore microtubule begins depolymerizing, its rate of depolymerization is not affected by Mps1. However, the distances traveled between pauses by poleward-migrating centromeres in *MPS1* mutants are shorter than in wild-type cells (Figure 5G) and the pauses are more frequent (Figure 5F). The pauses during poleward migration of the centromeres could represent losses of kinetochore-microtubule plus-end attachment or pauses in microtubule depolymerization, or both. Given that phosphorylation of Dam1 by Mps1 strengthens kinetochore attachments to plus ends (Shimogawa *et al.*, 2006; Meyer *et al.*, 2018), some of the pauses in *MPS1* mutants are probably due to failures in maintaining the kinetochore-plus-end connection. However, other results suggest that this is not the major defect. First, *MPS1* mutants exhibit low levels of the lagging chromosomes that are an indicator of a defect in attaching kinetochores to microtubules (Meyer *et al.*, 2013, 2018). Second, *MPS1* mutants exhibit a stuck-in-the-middle phenotype in which kinetochores maintain a very stable position in midspindle. This is unlike *DAM1* mutants, in which kinetochores and plus ends become uncoupled, or *NDC80* mutants, in which kinetochores do not attach to microtubules (Meyer *et al.*, 2018); in these two mutants the apparently unconnected centromeres move much more freely than in *MPS1* mutants. One explanation for the stuck-in-the-middle phenotype is that *MPS1* mutants may be defective in promoting the initiation of depolymerization of kinetochore-coupled MT plus ends. We propose that when a microtubule plus end attaches to a kinetochore, the proximity of the microtubule plus end–associated proteins to Mps1 allows Mps1 to phosphorylate key substrates associated with the plus end, changing their activity or localization in a way that favors microtubule catastrophe over rescue (Figure 6A). The identity of these Mps1 substrates and how their phosphorylation biases microtubule dynamics remains an important unanswered question.

The above model does not solve another unknown. Why is it that meiotic chromosome segregation is more vulnerable to defects in Mps1 activity than is mitosis? We offer three possible explanations. First, when mitosis begins, kinetochores are already attached to microtubules. In contrast, the chromosome paring process of meiotic prophase demands that kinetochores be released from microtubules for an extended time period. When meiotic prometaphase begins, the kinetochores are dispersed across the nucleus and are then gathered into the microtubule-dense region around the SPBs (clustering) just before the SPBs separate to form a spindle. Mps1 is required for this clustering (Meyer *et al.*, 2013). It may be that in the absence of clustering the formation of initial kinetochore-microtubule attachments on the nascent bipolar spindle is highly inefficient, leading to biorientation defects. A phenomenon similar to clustering, referred to as kinetochore retrieval, has been reported in *Schizosaccharomyces pombe* meiosis (Kakui *et al.*, 2013; Cojoc *et al.*, 2016). Here, mutations that lead to defects in meiotic kinetochore retrieval also result in subsequent biorientation defects, but it is difficult to know whether the segregation defects are purely due to the failure to cluster the dispersed meiotic kinetochores before spindle formation, or to other effects of the mutations.

Second, the vulnerability of meiotic cells to *MPS1* defects might lie in differences between meiotic and mitotic spindles. When yeast meiotic spindles form, most chromosomes are mono-oriented, with most chromosomes clustered near the older SPB (Meyer *et al.*, 2013). Mitosis starts in a similar way (Marco *et al.*, 2013). Thus, in both meiosis and mitosis, chromosomes that become bioriented have made their way to the spindle midzone from the pole. But yeast meiotic spindles are longer, possibly making them more dependent on processes that get them from the poles to the midzone (Meyer *et al.*, 2013). Movement from the pole to the midzone could be accomplished by pulling of the kinetochore by a long microtubule extending across the spindle from the opposite pole—a process that our results show is defective in *MPS1* mutants (Meyer *et al.*, 2013) both because failure to phosphorylate Dam1 results in defective end-on attachments and because processive poleward movements are defective in *MPS1* mutants. An alternate means to get to the midzone from the pole is by movement of chromosomes along microtubules

from that pole toward their plus ends. This chromosome gliding mechanism has been reported in *S. pombe* and animal cells but not budding yeast (Kapoor *et al.*, 2006; Windecker *et al.*, 2009; Akera *et al.*, 2015). In *S. pombe* the process involves proteins (Bub1, Bub3, Mad1, kinesin-5) whose kinetochore localization depends on Mps1 (Windecker *et al.*, 2009; Akera *et al.*, 2015) and is especially critical for chromosome biorientation in cells with long spindles. There is as yet no evidence that this mechanism is important in budding yeast. However, consistent with this model is the recent demonstration that *BUB1* and *BUB3* mutants, like *MPS1* mutants, both exhibit much higher levels of meiotic than mitotic segregation defects and missegregate homologous chromosomes to the older SPB in meiosis I, though not at the high levels seen in *MPS1* mutants (Cairo *et al.*, 2020).

Finally, the flexibility of the connections between homologous meiotic centromeres could make them vulnerable to deficiencies in Mps1. This is true of meiotic chromosomes across species and may explain the shared dependence on Mps1 in yeast, *Drosophila*, and zebrafish meioses. Mitotic sister kinetochores are arranged back-to-back, and tightly cohered. Bioriented attachments of sister chromatids are thus probably very quickly under tension and stabilized. In contrast, homologous meiotic kinetochores are connected by chiasmata and therefore a longer tether. This predicts that greater microtubule depolymerization is required in meiosis to separate the homologous kinetochores sufficiently that they are under tension. It may be that in the time interval between the formation of an initial bipolar attachment and the generation of stabilizing tension, one or both of the kinetochore-microtubule connections is lost, and the process must restart. This more challenging meiotic attachment process may render the cell vulnerable to any defects that diminish the efficiency of establishing kinetochore-microtubule attachments. The observation that in budding yeast, meiotic cells are much more sensitive to defects in the spindle checkpoint than are mitotic cells reinforces the idea that biorientation in meiosis faces greater hurdles than in mitosis (Shonn *et al.*, 2000; Cheslock *et al.*, 2005). But work remains to reveal the greatest vulnerabilities of the meiotic biorientation process and how the cell deals with them.

MATERIALS AND METHODS

Request a protocol through *Bio-protocol*.

Yeast strains and culture conditions

All strains are derivatives of two strains termed X and Y described previously (Dresser *et al.*, 1994). Strain genotypes are listed in Supplemental Tables S1 and S2. We used standard yeast culture methods (Amberg *et al.*, 2005). To induce meiosis, cells were grown in YP (yeast peptone) acetate to 4–4.5 × 10^7 cells per ml and then shifted to 1% potassium acetate at 10^8 cells per ml. Mitotic cells were grown in SD-TRP (complete synthetic defined medium missing tryptophan) media (Sunrise Science).

Genome modifications

Heterozygous and homozygous *CEN1-GFP* dots: An array of 256 *lac* operon operator sites on plasmid pJN2 was integrated near the *CEN1* locus (coordinates 153583–154854). *lacI-GFP* fusions under the control of P_{CYC1} and P_{DMC1} were also expressed in this strain to visualize the location of the *lacO* operator sites during meiosis as described in Meyer *et al.* (2013).

PCR-based methods were used to create complete deletions of ORFs and promoter insertions (Longtine *et al.*, 1998; Janke *et al.*, 2004). *spo11::KANMX, spo11::HIS3MX6, P_{GPD1}-GAL4(848)-ER-URA3::hphNT1, natNT2::P_{GAL1}-NDT80, KANMX::P_{GAL1}-NDT80, mps1::KANMX, TRP1::10Xmyc-mps1-as1 (= mps1-as1), mps1-R170S::his5, KANMX::P_{CLB2}-3HA-MPS1 (=mps1-md), KANMX::P_{CLB2}-3HA-NDC80 (= ndc80-md), KANMX::P_{CLB2}-3HA-DAM1 (= dam1-md),*and *SPC42-DsRed-URA3* strains were generated previously (Meyer *et al.*, 2013, 2018). The *mEos2-TUB1* strains were generated by inserting *pHIS3p:mEos2Tub1+3′UTR::TRP1* plasmid (https://www.addgene.org/50652/) in the *TUB1* locus as described (Markus *et al.*, 2015). The *SPC42-GFP-TRP1* strain was a gift from Mike Dresser, OMRF, Oklahoma (as described in Adams and Kilmartin, 1999).

Fluorescence microscopy

Long-term live cell imaging experiments (every 45–120 s for 3–4 h) were performed with CellAsic microfluidic flow chambers (www.emdmillipore.com) using Y04D plates with a flow rate of 5 psi. Images were collected with a Nikon Eclipse TE2000-E equipped with the Perfect Focus system, a Roper CoolSNAP HQ2 camera automated stage, an X-cite series 120 illuminator (EXFO) and NIS software. Images were processed and analyzed using NIS software. For the time-lapse imaging of *CEN1* movement, two different exposure programs were defined, depending on the presence (*SPO11*) or absence (*spo11Δ*) of chiasmata. In the presence of chiasmata, the intervals were every 2 min for 2 h and later every 5 min for 2 h (Supplemental Figure S2). Without chiasmata, images were acquired every 45 s or 2 min for 75 min followed by every 10 min for 3 h (Figures 2 and 3).

For monitoring movements of *CEN1-GFP* on monopolar spindles (side-by-side SPBs), following the release from prophase, centromeres were considered as unattached if they did not remain at a constant distance from the SPBs for at least four consecutive frames. Centromeres were considered to be attached if they stayed at a constant distance from the SPBs for at least three consecutive frames or moved incrementally in one direction. The beginning of clustering was defined when *CEN1-GFP* first reached a position within 0.5 μm of the SPB and remained within this distance for three consecutive frames. Traverses (*CEN1* crossing the spindle from one pole to the other) were counted only when the *CEN1-GFP* signal was overlapping with the SPB signal for at least one frame. Homologues were considered to be bioriented when the homologous *CEN1-GFP* signals were distinctly separated in two foci.

For high-speed live cell imaging, images were collected every 2 s for 5 min using a Roper CoolSNAP HQ2 camera on a Zeiss Axio Imager 7.1 microscope fitted with a 100×, NA1.4 plan-Apo objective (Carl Zeiss MicroImaging), an X-cite series 120 illuminator (EXFO), and a BNC555 pulse generator (Berkeley Nucleonics) to synchronize camera exposure with focusing movements and illumination. Cells from sporulating cultures were concentrated, spread across polyethyleneimine-treated coverslips, and then covered with a thin 1% agarose pad to anchor the cells to the coverslip. The coverslip was then inverted over a silicone rubber gasket attached to a glass slide. Thru-focus images were acquired as described previously and then deconvolved to provide a two-dimensional projected image for each acquisition (Conrad *et al.*, 2008). For the analysis of centromere movements on bipolar spindles, the coordinates of the two SPBs (labeled by *SPC42-GFP*) and the centromeres (marked by *CEN1-GFP*) were defined for each interval. To separate the movement inherent to spindle rotation inside the cells and the movement of *CEN1* on the spindle, a relative position for *CEN1* and the two SPBs was assigned for each interval. For one SPB (SPB1) this position was defined as being constant as $x = 0$ and $y = 0$. For the other SPB (SPB2), the position was defined as x = distance between the SPBs in each frame and $y = 0$. Finally, the relative position of

CEN1 was determined by the distance between *CEN1* and SPB1 and the angle formed between the axis SPB1-SPB2 and SPB1-*CEN1*. As the acquisitions were done in two dimensions, the impact of the spindle rotating in three dimensions was corrected by assuming that the spindle length remains the same or increases over time. Therefore, for instances in which the SPB1-SPB2 distances decreased in sequential frames, the value was corrected by replacing the SPB1-SPB2 distance with the prior maximum spindle length (dMax SPB1-SPB2). The magnitude of this correction was also then applied to correct the SPB1-*CEN1* distance; the following formula was applied for each interval: Distance SPB1-*CEN1* = Observed distance SPB1-*CEN1* x dMax SPB1-SPB2/Observed distance SPB1-SPB2. The velocity of *CEN1* movement on the spindle was calculated for each interval by adding the distance between interval $n - 1$ to $n + 1$ and dividing by the time interval (4 s). The median position for *CEN1* was determined in 5 min intervals for each cell by calculating the average position. The dispersion distance was determined for each interval by calculating the distance between *CEN1* and this average position. Cells with the following characteristics were selected to monitor poleward migration (Figure 5): The *CEN1* exhibited a migration of 0.9–1.2 µm to its final destination within 0.25 µm of one SPB. The angle of approach had to be within 15°C on the pole-to-pole spindle axis. The migrations started within the same half spindle of the destination SPB. During this 0.9–1.2 µm migration, the intermediate steps were considered poleward movement when the distance between SPB and *CEN1* from one interval to the other was decreasing and anti-poleward movement when increasing. The pauses and reversals of direction were determined as follows. First, the distance (D) between the final SPB destination and *CEN1* was calculated for each interval (frame). Second, the average distance for each sequential pair of steps was determined. Third, sequential positions in this sliding average were compared. If the distance between the SPB and *CEN1* was increasing ($D \geq 0$), the movement was considered to be paused/reversed. The number of consecutive poleward steps was determined as the number of consecutive steps showing continued decreasing distance ($D < 0$).

Measuring microtubule turnover

Microtubule turnover was evaluated in yeast cells expressing mEos2-Tub1, harvested from either log-phase vegetative cultures (in YPAD [yeast peptone adenine dextrose] medium [Amberg *et al.*, 2005]) or meiotic cultures. For meiotic experiments, cells in a pachytene arrest were induced to exit prophase by the addition of estradiol to the medium, using previously published methods (Meyer *et al.*, 2013). Where indicated, auxin (2 mM; Sigma Aldrich I5148-10G), $CuSO_4$ (200 µM; Sigma Aldrich 451657-10G), or 1-NMPP1 (5 µM; Calbiochem; 5 mM stock in dimethyl sulfoxide) were added to the medium at the time of prophase exit. One hour after prophase exit was induced, cells were concentrated, spread across polyethyleneimine-treated coverslips, and then covered with a thin 1% agarose pad to anchor the cells to the coverslip. The coverslip was then inverted over a silicone rubber gasket attached to a glass slide. Cells synchronously entering prometaphase were then subjected to imaging to measure microtubule turnover.

Cells were imaged using a 100×, NA 1.4 objective on a Zeiss Axio Observer inverted microscope equipped with a Yokogawa CSU-22 (Yokogawa) spinning disk, Mosaic (digital mirror device; Photonic Instruments/Andor), a Hamamatsu ORCA-Flash4.0LT (Hamamatsu Photonics), and Slidebook software (Intelligent Imaging Innovations). Photoconversion was achieved by targeting a selected area in half the spindle with filtered light from the HBO 100 via the Mosaic, and confocal GFP and RFP images were acquired at 15 s intervals for ~5 min. At each acquisition, we acquired seven images in the Z-dimension with 0.5 µm spacing. To quantify fluorescence dissipation after photoconversion, we measured pixel intensities within an area surrounding the region of highest fluorescence intensity and background subtracted using an area from the nonconverted half spindle using MetaMorph software. Fluorescence values were normalized to the first time point after photoconversion for each cell, and the average intensity at each time point was fitted to a single exponential decay curve $F = A \times \exp(-k \times t)$, using SigmaPlot (SYSTAT Software), where A represents the microtubule population with a decay rate of k, respectively. t is the time after photoconversion. For each experiment, we performed at least three biological replicates with at least three cells imaged per experiment. Cell numbers for each experiment are given in Table 1. Sample identity for scoring fluorescent signals was blinded. The half-life for the microtubule population was calculated as $\ln 2/k$. Graphs were prepared using GraphPad Prism. Graphs represent the averages and SEM for combined replicates.

ACKNOWLEDGMENTS

We thank Michael Dresser for providing OMRFQuant Imaging Software and Emma Lee for guidance in using Thru-focus Imaging methods. This project was supported by National Institutes of Health (NIH) grant R01GM110271, Oklahoma Center for the Advancement of Science and Technology grant HR17-115-3, and National Science Foundation Grant 8021974 awarded to D.S.D. and NIH grant R35GM126980 awarded to G.J.G.

REFERENCES

Abrieu A, Magnaghi-Jaulin L, Kahana JA, Peter M, Castro A, Vigneron S, Lorca T, Cleveland DW, Labbé JC (2001). Mps1 is a kinetochore-associated kinase essential for the vertebrate mitotic checkpoint. Cell 106, 83–93.

Adams IR, Kilmartin JV (1999). Localization of core spindle pole body (SPB) components during SPB duplication in Saccharomyces cerevisiae. J Cell Biol 145, 809–823.

Akera T, Goto Y, Sato M, Yamamoto M, Watanabe Y (2015). Mad1 promotes chromosome congression by anchoring a kinesin motor to the kinetochore. Nat Cell Biol 17, 1124–1133.

Amberg DC, Burke D, Strathern JN (2005). Methods in Yeast Genetics, Cold Spring Harbor, NY: CSHL Press.

Aravamudhan P, Goldfarb AA, Joglekar AP (2015). The kinetochore encodes a mechanical switch to disrupt spindle assembly checkpoint signalling. Nat Cell Biol 17, 868–879.

Asbury CL, Gestaut DR, Powers AF, Franck AD, Davis TN (2006). The Dam1 kinetochore complex harnesses microtubule dynamics to produce force and movement. Proc Natl Acad Sci USA 103, 9873–9878.

Biggins S, Severin FF, Bhalla N, Sassoon I, Hyman AA, Murray AW (1999). The conserved protein kinase Ipl1 regulates microtubule binding to kinetochores in budding yeast. Genes Dev 13, 532–544.

Cairo G, MacKenzie AM, Lacefield S (2020). Differential requirement for Bub1 and Bub3 in regulation of meiotic versus mitotic chromosome segregation. J Cell Biol 219, 1524.

Cheeseman IM, Anderson S, Jwa M, Green EM, Kang JS, Yates JR, Chan CSM, Drubin DG, Barnes G (2002). Phospho-regulation of kinetochore-microtubule attachments by the Aurora kinase Ipl1p. Cell 111, 163–172.

Chen J, Liao A, Powers EN, Liao H, Kohlstaedt LA, Evans R, Holly RM, Kim JK, Jovanovic M, Unal E (2020). Aurora B-dependent Ndc80 degradation regulates kinetochore composition in meiosis. Genes Dev 34, 209–225.

Cheslock PS, Kemp BJ, Boumil RM, Dawson DS (2005). The roles of MAD1, MAD2 and MAD3 in meiotic progression and the segregation of nonexchange chromosomes. Nat Genet 37, 756–760.

Chmátal L, Yang K, Schultz RM, Lampson MA (2015). Spatial regulation of kinetochore microtubule attachments by destabilization at spindle poles in meiosis I. Curr Biol 25, 1835–1841.

Cojoc G, Florescu A-M, Krull A, Klemm AH, Pavin N, Jülicher F, TolićIM (2016). Paired arrangement of kinetochores together with microtubule pivoting and dynamics drive kinetochore capture in meiosis I. Sci Rep 6, 25736.

Conrad MN, Lee C-Y, Chao G, Shinohara M, Kosaka H, Shinohara A, Conchello J-A, Dresser ME (2008). Rapid telomere movement in meiotic prophase is promoted by NDJ1, MPS3, and CSM4 and is modulated by recombination. Cell 133, 1175–1187.
Daum JR, Wren JD, Daniel JJ, Sivakumar S, McAvoy JN, Potapova TA, Gorbsky GJ (2009). Ska3 is required for spindle checkpoint silencing and the maintenance of chromosome cohesion in mitosis. Curr Biol 19, 1467–1472.
Dou Z, Sawagechi A, Zhang J, Luo H, Brako L, Yao XB (2003). Dynamic distribution of TTK in HeLa cells: insights from an ultrastructural study. Cell Res 13, 443–449.
Dresser ME, Ewing DJ, Harwell SN, Coody D, Conrad MN (1994). Nonhomologous synapsis and reduced crossing over in a heterozygous paracentric inversion in Saccharomyces cerevisiae. Genetics 138, 633–647.
Franco A, Meadows JC, Millar JBA (2007). The Dam1/DASH complex is required for the retrieval of unclustered kinetochores in fission yeast. J Cell Sci 120, 3345–3351.
Gachet Y, Reyes C, Courthéoux T, Goldstone S, Gay G, Serrurier C, Tournier S (2008). Sister kinetochore recapture in fission yeast occurs by two distinct mechanisms, both requiring Dam1 and Klp2. Mol Biol Cell 19, 1646–1662.
Gaitanos TN, Santamaria A, Jeyaprakash AA, Wang B, Conti E, Nigg EA (2009). Stable kinetochore–microtubule interactions depend on the Ska complex and its new component Ska3/C13Orf3. EMBO J 28, 1442–1452.
Gilliland WD, Wayson SM, Hawley RS (2005). The meiotic defects of mutants in the Drosophila mps1 gene reveal a critical role of Mps1 in the segregation of achiasmate homologs. Curr Biol 15, 672–677.
Godek KM, Kabeche L, Compton DA (2015). Regulation of kinetochore-microtubule attachments through homeostatic control during mitosis. Nat Rev Mol Cell Biol 16, 57–64.
Gorbsky GJ, Borisy GG (1989). Microtubules of the kinetochore fiber turn over in metaphase but not in anaphase. J Cell Biol 109, 653–662.
Grishchuk EL, Efremov AK, Volkov VA, Spiridonov IS, Gudimchuk N, Westermann S, Drubin D, Barnes G, McIntosh JR, Ataullakhanov FI (2008). The Dam1 ring binds microtubules strongly enough to be a processive as well as energy-efficient coupler for chromosome motion. Proc Natl Acad Sci USA 105, 15423–15428.
Hardwick KG, Weiss E, Luca FC, Winey M, Murray AW (1996). Activation of the budding yeast spindle assembly checkpoint without mitotic spindle disruption. Science 273, 953–956.
Hayden JH, Bowser SS, Rieder CL (1990). Kinetochores capture astral microtubules during chromosome attachment to the mitotic spindle: direct visualization in live newt lung cells. J Cell Biol 111, 1039–1045.
Howell BJ, Moree B, Farrar EM, Stewart S, Fang G, Salmon ED (2004). Spindle checkpoint protein dynamics at kinetochores in living cells. Curr Biol 14, 953–964.
Humphrey L, Felzer-Kim I, Joglekar AP (2018). Stu2 acts as a microtubule destabilizer in metaphase budding yeast spindles. Mol Biol Cell 29, 247–255.
Janke C, Magiera MM, Rathfelder N, Taxis C, Reber S, Maekawa H, Moreno-Borchart A, Doenges G, Schwob E, Schiebel E, Knop M (2004). A versatile toolbox for PCR-based tagging of yeast genes: new fluorescent proteins, more markers and promoter substitution cassettes. Yeast 21, 947–962.
Jones MH, Huneycutt BJ, Pearson CG, Zhang C, Morgan G, Shokat K, Bloom K, Winey M (2005). Chemical genetics reveals a role for Mps1 kinase in kinetochore attachment during mitosis. Curr Biol 15, 160–165.
Kakui Y, Sato M, Okada N, Toda T, Yamamoto M (2013). Microtubules and Alp7-Alp14 (TACC-TOG) reposition chromosomes before meiotic segregation. Nat Cell Biol 15, 786–796.
Kapoor TM, Lampson MA, Hergert P, Cameron L, Cimini D, Salmon ED, McEwen BF, Khodjakov A (2006). Chromosomes can congress to the metaphase plate before biorientation. Science 311, 388–391.
Kitamura E, Tanaka K, Kitamura Y, Tanaka TU (2007). Kinetochore microtubule interaction during S phase in Saccharomyces cerevisiae. Genes Dev 21, 3319–3330.
Klapholz S, Waddell CS, Esposito RE (1985). The role of the SPO11 gene in meiotic recombination in yeast. Genetics 110, 187–216.
Koch LB, Opoku KN, Deng Y, Barber A, Littleton AJ, London N, Biggins S, Asbury CL (2019). Autophosphorylation is sufficient to release Mps1 kinase from native kinetochores. Proc Natl Acad Sci USA 116, 17355–17360.
Kosco KA, Pearson CG, Maddox PS, Wang PJ, Adams IR, Salmon ED, Bloom K, Huffaker TC (2001). Control of microtubule dynamics by Stu2p is essential for spindle orientation and metaphase chromosome alignment in yeast. Mol Biol Cell 12, 2870–2880.
Lampert F, Hornung P, Westermann S (2010). The Dam1 complex confers microtubule plus end-tracking activity to the Ndc80 kinetochore complex. J Cell Biol 189, 641–649.
Lampson MA, Grishchuk EL (2017). Mechanisms to avoid and correct erroneous kinetochore-microtubule attachments. Biology 6, 1.
Loidl J, Klein F, Scherthan H (1994). Homologous pairing is reduced but not abolished in asynaptic mutants of yeast. J Cell Biol 125, 1191–1200.
Longtine MS, McKenzie A, Demarini DJ, Shah NG, Wach A, Brachat A, Philippsen P, Pringle JR (1998). Additional modules for versatile and economical PCR-based gene deletion and modification in Saccharomyces cerevisiae. Yeast 14, 953–961.
Magidson V, O'Connell CB, Lončarek J, Paul R, Mogilner A, Khodjakov A (2011). The spatial arrangement of chromosomes during prometaphase facilitates spindle assembly. Cell 146, 555–567.
Marco E, Dorn JF, Hsu P-H, Jaqaman K, Sorger PK, Danuser G (2013). S. cerevisiae chromosomes biorient via gradual resolution of syntely between S phase and anaphase. Cell 154, 1127–1139.
Markus SM, Omer S, Baranowski K, Lee W-L (2015). Improved plasmids for fluorescent protein tagging of microtubules in Saccharomyces cerevisiae. Traffic 16, 773–786.
Merdes A, De Mey J (1990). The mechanism of kinetochore-spindle attachment and polewards movement analyzed in PtK2 cells at the prophase-prometaphase transition. Eur J Cell Biol 53, 313–325.
Meyer RE, Brown J, Beck L, Dawson DS (2018). Mps1 promotes chromosome meiotic chromosome biorientation through Dam1. Mol Biol Cell 29, 479–489.
Meyer RE, Chuong HH, Hild M, Hansen CL, Kinter M, Dawson DS (2015). Ipl1/Aurora-B is necessary for kinetochore restructuring in meiosis I in Saccharomyces cerevisiae. Mol Biol Cell 26, 2986–3000.
Meyer RE, Kim S, Obeso D, Straight PD, Winey M, Dawson DS (2013). Mps1 and Ipl1/Aurora B act sequentially to correctly orient chromosomes on the meiotic spindle of budding yeast. Science 339, 1071–1074.
Miller MP, Asbury CL, Biggins S (2016). A TOG protein confers tension sensitivity to kinetochore-microtubule attachments. Cell 165, 1428–1439.
Miller MP, Evans RK, Zelter A, Geyer EA, MacCoss MJ, Rice LM, Davis TN, Asbury CL, Biggins S (2019). Kinetochore-associated Stu2 promotes chromosome biorientation in vivo. PLoS Genet 15, e1008423.
Miller MP, Unal E, Brar GA, Amon A (2012). Meiosis I chromosome segregation is established through regulation of microtubule-kinetochore interactions. eLife 1, e00117.
Monje-Casas F, Prabhu VR, Lee BH, Boselli M, Amon A (2007). Kinetochore orientation during meiosis is controlled by Aurora B and the monopolin complex. Cell 128, 477–490.
Nicklas RB (1997). How cells get the right chromosomes. Science 275, 632–637.
Pearson CG, Maddox PS, Zarzar TR, Salmon ED, Bloom K (2003). Yeast kinetochores do not stabilize Stu2p-dependent spindle microtubule dynamics. Mol Biol Cell 14, 4181–4195.
Podolski M, Mahamdeh M, Howard J (2014). Stu2, the budding yeast XMAP215/Dis1 homolog, promotes assembly of yeast microtubules by increasing growth rate and decreasing catastrophe frequency. J Biol Chem 289, 28087–28093.
Poss KD, Nechiporuk A, Stringer KF, Lee C, Keating MT (2004). Germ cell aneuploidy in zebrafish with mutations in the mitotic checkpoint gene mps1. Genes Dev 18, 1527–1532.
Powers AF, Franck AD, Gestaut DR, Cooper J, Gracyzk B, Wei RR, Wordeman L, Davis TN, Asbury CL (2009). The Ndc80 kinetochore complex forms load-bearing attachments to dynamic microtubule tips via biased diffusion. Cell 136, 865–875.
Rieder CL, Alexander SP (1990). Kinetochores are transported poleward along a single astral microtubule during chromosome attachment to the spindle in newt lung cells. J Cell Biol 110, 81–95.
Sarangapani KK, Duro E, Deng Y, Alves Fde L, Ye Q, Opoku KN, Ceto S, Rappsilber J, Corbett KD, Biggins S, *et al.* (2014). Sister kinetochores are mechanically fused during meiosis I in yeast. Science 346, 248–251.
Schmidt JC, Arthanari H, Boeszoermenyi A, Dashkevich NM, Wilson-Kubalek EM, Monnier N, Markus M, Oberer M, Milligan RA, Bathe M, *et al.* (2012). The kinetochore-bound Ska1 complex tracks depolymerizing microtubules and binds to curved protofilaments. Dev Cell 23, 968–980.
Shimogawa MM, Graczyk B, Gardner MK, Francis SE, White EA, Ess M, Molk JN, Ruse C, Niessen S, Yates JR 3rd, *et al.* (2006). Mps1 phosphorylation of Dam1 couples kinetochores to microtubule plus ends at metaphase. Curr Biol 16, 1489–1501.

Shonn MA, McCarroll R, Murray AW (2000). Requirement of the spindle checkpoint for proper chromosome segregation in budding yeastmeiosis. Science 289, 300–303.
Straight AF, Belmont AS, Robinett CC, Murray AW (1996). GFP tagging of budding yeast chromosomes reveals that protein-protein interactions can mediate sister chromatid cohesion. Curr Biol 6, 1599–1608.
Straight PD, Giddings TH, Winey M (2000). Mps1p regulates meiotic spindle pole body duplication in addition to having novel roles during sporulation. Mol Biol Cell 11, 3525–3537.
Tanaka K, Kitamura E, Kitamura Y, Tanaka TU (2007). Molecular mechanisms of microtubule-dependent kinetochore transport toward spindle poles. J Cell Biol 178, 269–281.
Tanaka K, Mukae N, Dewar H, van Breugel M, James EK, Prescott AR, Antony C, Tanaka TU (2005). Molecular mechanisms of kinetochore capture by spindle microtubules. Nature 434, 987–994.
Tanaka TU (2010). Kinetochore-microtubule interactions: steps towards bi-orientation. EMBO J 29, 4070–4082.
Tanaka TU, Rachidi N, Janke C, Pereira G, Galova M, Schiebel E, Stark MJR, Nasmyth K (2002). Evidence that the Ipl1-Sli15 (Aurora kinase-INCENP) complex promotes chromosome bi-orientation by altering kinetochore-spindle pole connections. Cell 108, 317–329.
Umbreit NT, Miller MP, Tien JF, Cattin Ortolá J, Gui L, Lee KK, Biggins S, Asbury CL, Davis TN (2014). Kinetochores require oligomerization of Dam1 complex to maintain microtubule attachments against tension and promote biorientation. Nat Commun 5, 4951.
Volkov VA, Zaytsev AV, Gudimchuk N, Grissom PM, Gintsburg AL, Ataullakhanov FI, McIntosh JR, Grishchuk EL (2013). Long tethers provide high-force coupling of the Dam1 ring to shortening microtubules. Proc Natl Acad Sci USA 110, 7708–7713.
Weiss E, Winey M (1996). The Saccharomyces cerevisiae spindle pole body duplication gene MPS1 is part of a mitotic checkpoint. J Cell Biol 132, 111–123.
Welburn JPI, Grishchuk EL, Backer CB, Wilson-Kubalek EM, Yates JR, Cheeseman IM (2009). The human kinetochore Ska1 complex facilitates microtubule depolymerization-coupled motility. Dev Cell 16, 374–385.
Westermann S, Wang H-W, Avila-Sakar A, Drubin DG, Nogales E, Barnes G (2006). The Dam1 kinetochore ring complex moves processively on depolymerizing microtubule ends. Nature 440, 565–569.
Windecker H, Langegger M, Heinrich S, Hauf S (2009). Bub1 and Bub3 promote the conversion from monopolar to bipolar chromosome attachment independently of shugoshin. EMBO Rep 10, 1022–1028.
Winey M, Morgan GP, Straight PD, Giddings TH, Mastronarde DN (2005). Three-dimensional ultrastructure of Saccharomyces cerevisiae meiotic spindles. Mol Biol Cell 16, 1178–1188.
Wolyniak MJ, Blake-Hodek K, Kosco K, Hwang E, You L, Huffaker TC (2006). The regulation of microtubule dynamics in Saccharomyces cerevisiae by three interacting plus-end tracking proteins. Mol Biol Cell 17, 2789–2798.
Zhai Y, Kronebusch PJ, Borisy GG (1995). Kinetochore microtubule dynamics and the metaphase-anaphase transition. J Cell Biol 131, 721–734.